

What limits the power conversion efficiency of GaN-based lasers?

Joachim Piprek*

NUSOD Institute LLC, Newark, DE 19714-7204, United States

Abstract: Shuji Nakamura predicted in his Nobel lecture that GaN-based blue laser diodes are the future of solid state lighting. However, GaN-lasers still exhibit less than 40% electrical-to-optical power conversion efficiency while some blue LEDs exceed 80% and some GaAs-based infrared lasers exceed 70%. This talk investigates the reasons behind the efficiency limitation of GaN-based lasers and proposes an improved efficiency analysis method.

Keywords: high-power laser diode, InGaN/GaN, efficiency, Auger recombination, resistance, hole mobility

1. INTRODUCTION

In 2014, Nobel laureate Shuji Nakamura predicted that GaN-based laser diodes are the future of solid state lighting (SSL).¹ Such blue light emitting lasers are already utilized in the headlights of some high-end cars. However, the main driving force behind the current SSL boom is the promise of high energy efficiency. Some blue light-emitting diodes (LEDs) achieve more than 80% electrical-to-optical power conversion efficiency (PCE),^{2,3} but the highest PCE reported for GaN-based laser diodes is still below 40%.^{4,5,6} In comparison, some infrared light emitting InGaAs/GaAs lasers achieve more than 70% at room temperature.⁷ We here investigate the reasons for the efficiency limitation of GaN-lasers by numerical analysis of measured laser characteristics.

The light output power $P(I)$ of a semiconductor laser is typically described as function of the injected current I by

$$P(I) = \frac{h\nu}{q} \eta_i \frac{\alpha_m}{\alpha_m + \alpha_i} (I - I_{th}) \quad (1)$$

with the photon energy $h\nu$, the electron charge q , the differential internal quantum efficiency η_i , the internal absorption loss α_i , and the mirror loss α_m . The threshold current $I_{th} = I_{SRH} + I_{spon} + I_{Aug}$ compensates for carrier losses in the active layers due to Shockley-Read-Hall (SRH) recombination, spontaneous photon emission, and Auger recombination, respectively. Under ideal conditions without self-heating, these carrier losses do not rise above threshold since the carrier density n_{th} remains constant (clamped). The current fraction consumed by stimulated recombination is given by $I_{stim} = \eta_i (I - I_{th})$, where η_i accounts for the carrier leakage current I_{leak} that feeds recombination processes outside the active layer. Note that we here neglect the contribution of leakage to the threshold current, which will be validated below. The total current has five components: $I = I_{SRH} + I_{spon} + I_{Aug} + I_{leak} + I_{stim} = I_{th} + I_{leak} + I_{stim}$. The power conversion efficiency is defined as ratio of light output power to electrical input power IV (V - bias)

$$\eta_{PCE}(I) = \frac{h\nu}{qV} \eta_i \eta_o \frac{I - I_{th}}{I} = \eta_e \eta_i \eta_o \eta_{th} \quad (2)$$

including the electrical efficiency $\eta_e = h\nu/qV$, the optical efficiency $\eta_o = \alpha_m/(\alpha_m + \alpha_i)$, and the threshold current efficiency $\eta_{th} = (I - I_{th})/I$. However, this popular analytical model becomes problematic when the laser experiences relevant self-heating which leads to a sub-linear $P(I)$ characteristic. As the internal laser temperature rises with increasing current, the photon energy $h\nu(I)$ red-shifts due to band-gap shrinkage, the threshold current $I_{th}(I)$ rises together with the threshold carrier density $n_{th}(I)$ due to declining material gain in the active layers, the internal efficiency $\eta_i(I)$ may drop due to increasing carrier leakage, and the optical efficiency $\eta_o(I)$ may suffer from rising internal absorption $\alpha_i(I)$. The change $\alpha_i(I)$ was neglected in our previous investigation.⁸ Published efficiency analyses of high-power laser diodes typically

* piprek@nusod.org; phone 1-302-565-4945; www.nusod.org

assume a constant threshold current.⁷ Here, we consider all of the above variations and analyze their influence on the power conversion efficiency.

2. MODEL AND PARAMETERS

The numerical laser model is based on the LASTIP simulation software.⁹ It self-consistently computes carrier transport, the wurtzite electron band structure of strained InGaN quantum wells (QWs), stimulated photon emission, wave guiding, and heat flow. The transport model includes drift and diffusion of electrons and holes, Fermi statistics, built-in polarization and thermionic emission at hetero-interfaces, as well as all relevant radiative and non-radiative recombination mechanisms. Schrödinger and Poisson equations are solved iteratively in order to account for the QW deformation with changing device bias (quantum-confined Stark effect). More details on the employed laser models can be found elsewhere.¹⁰

Our experimental reference device is a 405 nm Fabry-Perot laser exhibiting a record-high light output power of $P=7.2\text{W}$ at $I=4\text{A}$ input current and $V=6.3\text{V}$ bias in continuous-wave (CW) operation at room temperature.⁶ The high output power was mainly accomplished by reducing the thermal resistance to about 7K/W ,¹¹ and by inserting thick undoped GaN waveguide layers that reduce the modal overlap with the strongly absorbing p-doped layers. Vertical waveguide structure and lasing mode are illustrated in Fig. 1. The epitaxial laser structure given in Tab. 1. The p-AlGaIn electron blocking layer (EBL) was moved to the p-side edge of the GaN waveguide in order to minimize the bias.⁶ The multi-quantum well (MQW) active region features two 7.5nm thick InGaIn quantum wells. The cavity length is $1200\mu\text{m}$ and the ridge width $12\mu\text{m}$. The front/back facet reflectance is $0.056/0.95$.

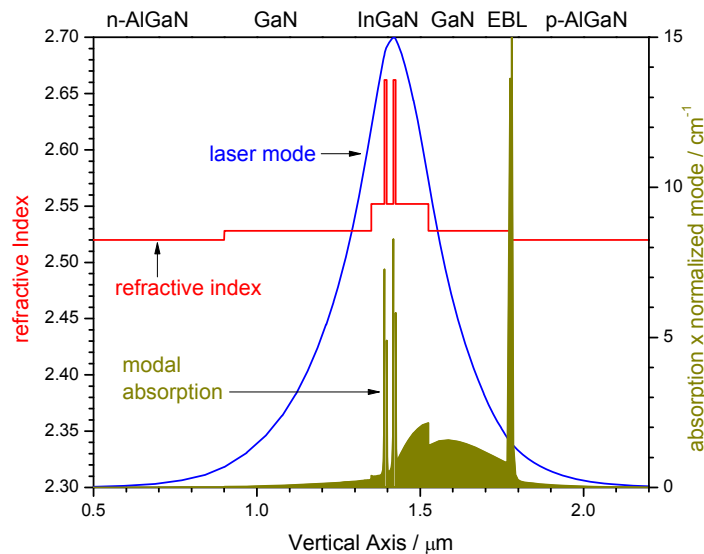


Fig. 1: Vertical profiles of the refractive index (red),⁶ lasing mode (normalized, blue) and modal absorption (dark yellow) as calculated at $I=4.3\text{A}$. The p-side waveguide layers cause two thirds of the free-carrier absorption due to leakage (cf. Fig. 6).

Crucial material parameters are obtained by reproducing the published laser performance (Fig. 2). The threshold current is mainly controlled by QW Auger recombination with a temperature-independent coefficient $C = 4.3 \cdot 10^{-30}\text{cm}^6/\text{s}$, which lies within the range of measured numbers.¹² Defect-related Shockley-Read-Hall (SRH) recombination has a negligible impact despite the relatively short SRH lifetime of 20 ns assumed inside the QWs. The slope of $P(I)$ is mainly limited by free-carrier absorption.⁶ We here adopt a first-principle model for phonon-assisted free-carrier absorption which results in an absorption cross section of about $0.6 \cdot 10^{-18}\text{cm}^2$ for our case, which is nearly identical for electrons and holes.¹³ Without further fitting, this model gives good agreement with the measured $P(I)$ characteristic in Fig. 2. This figure also shows the simulation result without Auger recombination and without absorption loss, respectively, both of which obviously limit the output power significantly at higher current.

Layer	Composition	Thickness	Index
p-cladding	Al _{0.026} GaN:Mg	660 nm	2.520
p-EBL	Al _{0.36} GaN:Mg	5 nm	2.350
waveguide	GaN	250 nm	2.528
waveguide	In _{0.008} GaN	100 nm	2.522
quantum well	In _{0.066} GaN	7.5nm	2.622
barrier	In _{0.008} GaN	20 nm	2.522
quantum well	In _{0.066} GaN	7.5 nm	2.622
waveguide	In _{0.008} GaN	40 nm	2.522
waveguide	GaN	450 nm	2.528
n-cladding	Al _{0.026} GaN:Si	900 nm	2.520

Tab. 1: Simulated laser structure.⁶ The influence of the substrate and the contacts is added as external electrical resistance and external thermal conductance.

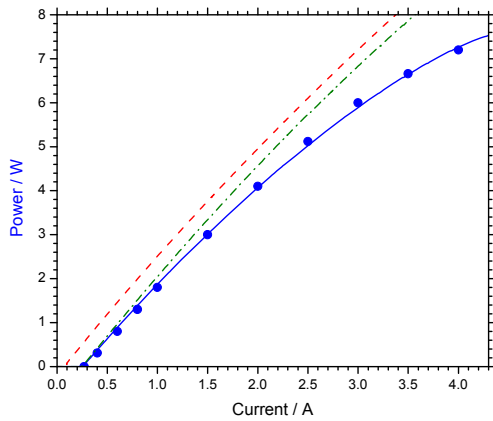


Fig. 2: Comparison between power-current measurements (dots)⁶ and simulations (lines). The red dashed line is simulated without Auger recombination and the green dash-dot line without absorption loss.

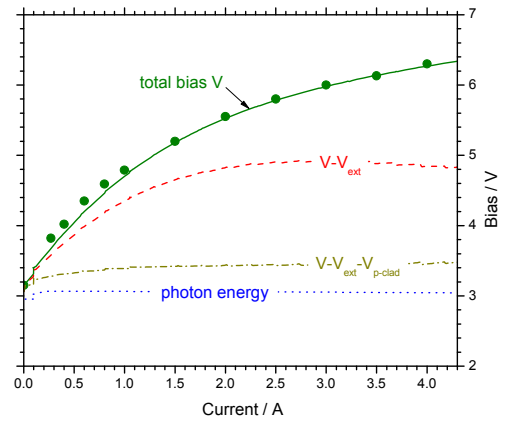


Fig. 3: Comparison between bias-current measurements (dots)⁶ and simulations (lines). The dashed gives the bias without external contribution from contacts and substrate. The dash-dot line additionally excludes the p-cladding resistance. The dotted line gives the minimum bias corresponding to the photon energy.

The calculated internal temperature rise is $\Delta T=138\text{K}$ at $I=4.3\text{A}$ based on the measured thermal resistance of $\Delta T/(IV-P) = 7\text{ K/W}$.¹¹ This temperature rise nearly quadruples the density of free holes in the p-AlGaIn cladding layer, due to the large Mg acceptor ionization energy of about 180meV .¹⁴ At room temperature, we calibrate the (unknown) Mg acceptor density to match the reported hole density of 10^{18} cm^{-3} .⁶ The p-AlGaIn hole mobility ($2\text{ cm}^2/\text{Vs}$) and external series resistance (0.35Ω) are then adjusted to achieve agreement with the bias measurement in Fig. 3. The external resistance accounts for all contributions outside the simulated region, including substrate and contacts. Both numbers are not reported for this laser but quite reasonable.¹⁵ Thus, the sub-linearity of the measured bias-current characteristic can be explained by thermal activation of holes in the p-AlGaIn cladding layer. The excess bias above the photon energy is initially dominated by the temperature-sensitive p-AlGaIn cladding resistance but the temperature-independent external resistance starts to dominate at higher current.

3. ANALYSIS AND DISCUSSION

Based on the good agreement with measurements, we now study internal processes revealed by the simulation in order to identify efficiency limiting mechanisms. Most importantly, the QW material gain is reduced at higher temperature due to

the wider spreading of the Fermi distribution of electrons and holes.¹⁶ In order to maintain the required threshold gain, the QW carrier density needs to rise. Figure 4 shows that the QW carrier density more than doubles at high power, but it remains constant without self-heating, as expected. Consequently, self-heating triggers a strong threshold current rise $I_{th}(I)$ since the Auger recombination rate increases with the third power of the carrier density (Fig. 5). The threshold current sums up all QW recombination processes that do not contribute to stimulated emission of photons, i.e., Auger recombination, spontaneous emission, and SRH recombination.

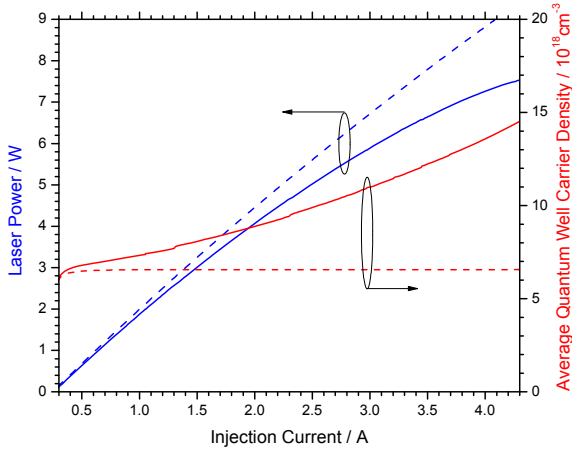


Fig. 4: Laser power and average QW carrier density as calculated with (solid) and without (dashed) self-heating above lasing threshold.

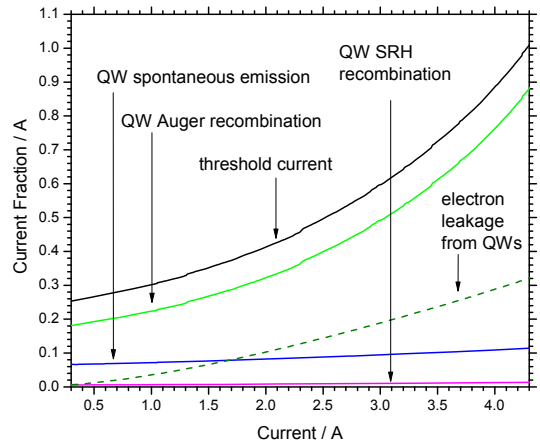


Fig. 5: Calculated fractions of the total current above lasing threshold.

The leakage current in Fig. 5 is obtained by integrating over all recombination processes outside the QWs. It is caused by electrons escaping from the QWs into the p-side waveguide layers, where they recombine with holes. Leakage beyond the EBL is not observed. The leakage current is negligibly small at the initial lasing threshold near room temperature, as assumed in the introduction, so that leakage is only reflected by the differential internal quantum efficiency $\eta_i = I_{stim} / (I_{stim} + I_{leak})$. This way, the effect of leakage and Auger recombination can be clearly separated in the efficiency analysis. Leaked electrons accumulate together with holes in the p-side waveguide layers (Fig. 6). EBL doping and polarization field cause a spike in the hole density. This is also reflected in the modal absorption profile in Fig. 1 which amounts to a total modal loss of $\alpha_i = 2.1/\text{cm}$ at $I = 4.3\text{A}$, in good agreement with measurements.⁶

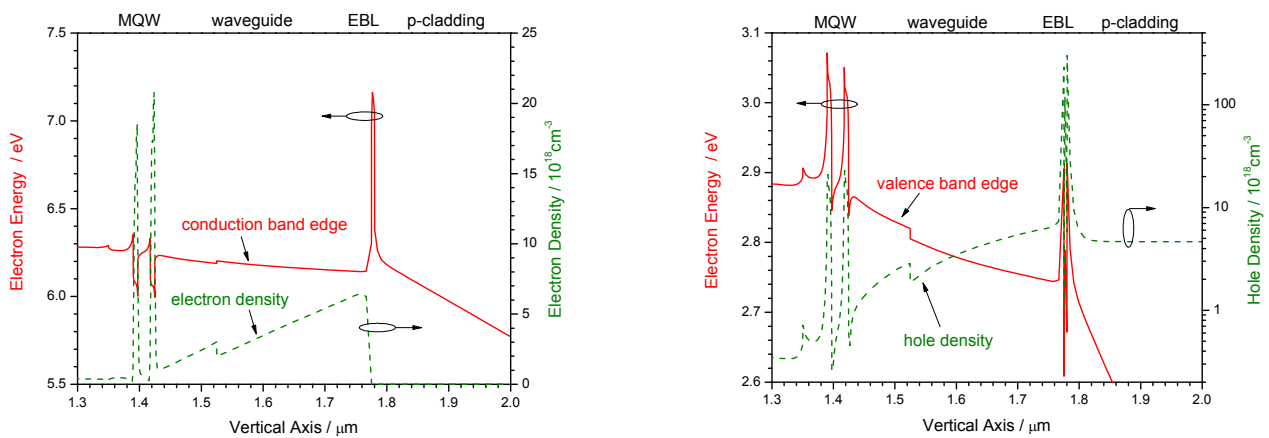


Fig. 6: Vertical profiles of band edges (solid) and carrier concentrations (dashed) at $I=4.3\text{A}$.

Figure 7 plots the efficiencies calculated with and without self-heating. The differential efficiency η_i representing the electron leakage has the weakest influence. It hardly changes with increasing current and it is not much affected by the self-heating. This is somewhat surprising but can be understood using Fig. 5 in which leakage accounts for less than 7% of the total current. Correspondingly, free-carrier absorption losses are also not much affected by the temperature. The optical efficiency η_o declines with increasing current but remains above the threshold current efficiency. The latter dominates at low power. It reflects the influence of Auger recombination which rises strongly with self-heating. However, the main high-power efficiency limitation originates in the decline of the electrical efficiency η_e due to the rising bias. At lower current, this is mainly attributed to the poor hole conductivity in the p-cladding layer which is even lower without self-heating. But the p-cladding contribution to the bias saturates with higher temperature, due to the thermal activation of additional holes, so that the temperature independent part of the series resistance dominates at higher current (see Fig. 3). Overall, the high-power PCE is slightly improved by the self heating in Fig. 7 since the enhanced hole conductivity counteracts the rising Auger recombination.

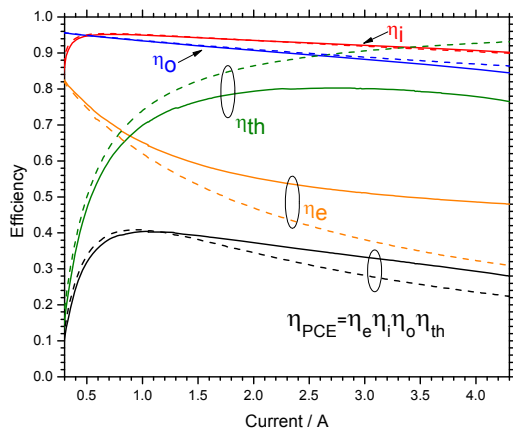


Fig. 7: Efficiencies vs. current above lasing threshold (η_{PCE} – power conversion efficiency, η_e – electrical efficiency, η_o – optical efficiency, η_i – injection efficiency, η_{th} – threshold current efficiency, solid/dashed: with/without self-heating).

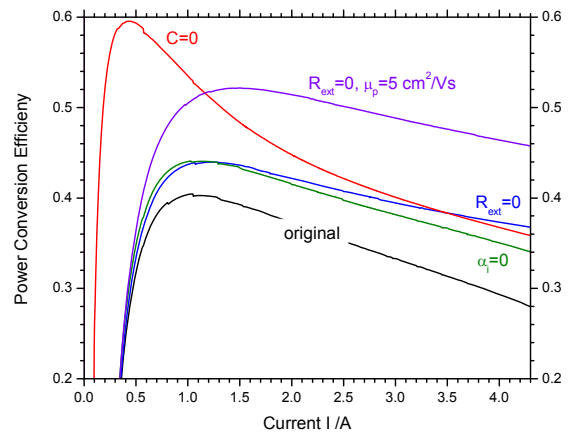


Fig. 8: Power conversion efficiency vs. current for different variations of simulation parameters as described in the text.

Figure 8 shows the PCE after exclusion of key loss mechanisms from the simulation. Auger recombination has the strongest effect at low current but it is hardly avoidable in reality. Elimination of absorption has only a modest effect as the internal loss is already very low in this laser. Removal of the external resistance facilitates a somewhat higher PCE. Combined with a modest p-AlGaIn mobility enhancement to $5 \text{ cm}^2/\text{Vs}$, it increases the PCE to about 50% even at higher current.

The most efficient laser diodes today are based on GaAs and some reach $\eta_{PCE} > 70\%$ in CW operation at room temperature.⁷ Their thermal resistance is similar to GaN-lasers, but their internal absorption loss is often well below $1/\text{cm}$. InGaAs/GaAs lasers don't suffer from the high QW polarization field that separates electrons and holes in InGaN/GaN QWs. The QW Auger recombination is somewhat stronger in GaAs-lasers; however, their threshold carrier density is much lower than in GaN-lasers. Most importantly, the series resistance reported for GaAs-lasers ($20\text{m}\Omega$)⁷ is more than one order of magnitude smaller than with GaN-lasers.

4. SUMMARY

The large series resistance is the main reason for the low power conversion efficiency of GaN-based lasers. However, Auger recombination gains increasing influence at high power due to the thermally induced rise of the threshold carrier density. The lasing power is also limited by enhanced free-carrier absorption due to electron leakage into the p-side waveguide layer.

REFERENCES

- ¹ Nakamura, S., "Background story of the invention of efficient blue InGaN light emitting diodes (Nobel Lecture)," *Ann. Phys.* 527, 335-349 (2015)
- ² Hurni, C.A., A. David, M.J. Cich, R. I. Aldaz, et al., "Bulk GaN flip-chip violet light-emitting diodes with optimized efficiency for high-power operation," *Appl. Phys. Lett.* 106, 031101 (2015)
- ³ Kimura, S., H. Yoshida, K. Uesugi, T. Ito, A. Okada, and S. Nunoue, "Performance enhancement of blue light-emitting diodes with InGaN/GaN multi-quantum wells grown on Si substrates by inserting thin AlGaIn interlayers." *J. Appl. Phys.* 120, 113104 (2016)
- ⁴ Raring, J. W., "Laser diodes for next generation light sources," Presented at DOE SSL R&D Workshop, Raleigh, NC, Feb. 2016.
- ⁵ Loeffler, A., C. Eichler, J. Mueller, S. Gerhard, et al., "InGaN power laser chips in a novel 50W multi-die package," *Proc. SPIE* 9363, 936318 (2015)
- ⁶ Kawaguchi, M., O. Imafuji, S. Nozaki, H. Hagino, et al., "Optical-loss suppressed InGaN laser diodes using undoped thick waveguide structure," *Proc. SPIE* 9748, 974818 (2016)
- ⁷ Crump, P., G. Erbert, H. Wenzel, C. Frevert, et al., "Efficient High-Power Laser Diodes," *J. Sel. Top. Quantum Electron.* 19, 1501211 (2013)
- ⁸ Piprek, J., "Analysis of efficiency limitations in high-power InGaN/ GaN laser diodes," *Opt. Quant. Electron.* 48, 471 (2016)
- ⁹ Crosslight Software Inc., Vancouver, Canada
- ¹⁰ Piprek, J., *Semiconductor Optoelectronic Devices: Introduction to Physics and Simulation*, Academic Press, San Diego (2003)
- ¹¹ Nozaki, S., S. Yoshida, K. Yamanaka, O. Imafuji, et al., "High-power and high-temperature operation of an InGaN laser over 3W at 85 °C using a novel double-heat-flow packaging technology," *Jpn. J. Appl. Phys.* 55, 04EH05 (2016)
- ¹² Piprek, J., F. Roemer, B. Witzigmann, "On the uncertainty of the Auger recombination coefficient extracted from InGaN/GaN light-emitting diode efficiency droop measurements," *Appl. Phys. Lett.* 106, 101101 (2015)
- ¹³ Kioupakis, E., P. Rinke, and C.G. Van de Walle, "Determination of Internal Loss in Nitride Lasers from First Principles" *App. Phys. Express* 3, 082101 (2010)
- ¹⁴ Piprek, J., "How to decide between competing efficiency droop models for GaN-based light-emitting diodes," *Appl. Phys. Lett.* 107, 031101 (2015)
- ¹⁵ Yonkee, B. P. , E. C. Young, C. Lee, J.T. Leonard, et al., "Demonstration of a III-nitride edge-emitting laser diode utilizing a GaN tunnel junction contact," *Optics Express* 24, 256556 (2016)
- ¹⁶ Piprek, J., "What limits the efficiency of high-power InGaN/GaN lasers?", to be published in *J. Quant. Electron.* (2017)